Diagnosing Fuel ρR and ρR Asymmetries in Cryogenic DT Implosions Using Charged-Particle Spectrometry on OMEGA

Introduction

Cryogenic deuterium–tritium (DT) capsules are routinely imploded on LLE's OMEGA Laser System.[1] These implosions are hydrodynamically equivalent to the baseline direct-drive-ignition design for the National Ignition Facility (NIF)[2] to allow for experimental validation of the design prior to the first ignition experiments at the NIF. The design consists of a cryogenic-DT-fuel layer inside a thin spherical ablator,[3] which is compressed quasi-isentropically to minimize the laser energy required to achieve ignition conditions. If the capsule is sufficiently compressed, the high areal density (ρR) of the cryogenic DT fuel can support a propagating thermonuclear burn wave due to local bootstrap heating by the DT-alpha particles. Maximizing ρR for a given on-capsule laser energy is therefore very important. Determining ρR is also important for assessing implosion performance during all stages of development from energy-scaled cryogenic DT implosions on OMEGA to cryogenic fizzles to ignited implosions on the NIF. Determining fuel ρR in moderate-ρR (100 to 200 mg/cm^2) cryogenic DT implosions has been challenging since it requires the development of new spectrometry techniques and analysis methods. A new type of neutron spectrometer, the magnetic recoil spectrometer (MRS),[4–6] has been built, installed, and calibrated on OMEGA to measure primarily the down-scattered DT neutron spectrum, from which ρR of the fuel can be directly inferred. Another MRS is currently being developed to diagnose high-ρR cryogenic DT-capsule implosions on the NIF.

This article describes a complementary method for analyzing the spectral shape of knock-on deuterons (KOd's), elastically scattered by primary DT neutrons, from which ρR can be inferred for values up to ~200 mg/cm^2. This new analysis method, which uses Monte Carlo modeling[7] of a cryogenic DT implosion, significantly improves, in two fundamental ways, the existing analysis method, which uses a relatively simple implosion model to relate the fuel ρR to the KOd yield in the high-energy peak.[8–10] First, it is not affected by significant spatial-yield variations, which degrade the diagnosis of fuel ρR (spatial-yield variations of about ±20% are typically observed). Secondly, it does not break down when the fuel ρR exceeds ~70 mg/cm^2. Modeling the actual shape of the KOd spectrum is therefore a more powerful method than the yield method for diagnosing the fuel ρR in cryogenic DT implosions.

The following sections describe the analysis method used to model the KOd spectrum, from which a ρR of the fuel can be inferred for a cryogenic DT implosion; present the experiments, data analysis, and results; and summarize the article.

Diagnosing Fuel ρR in Moderate-ρR Cryogenic DT Implosions Using Knock-On Deuterons

Fuel ρR in DT-filled CH-capsule implosions has been diagnosed routinely at the Omega Laser Facility for more than a decade.[8–10] In those experiments, two magnet-based charged-particle spectrometers (CPS's)[11] have been used to measure the KOd spectrum in two different directions. With the recent implementation of the MRS, a third measurement of the KOd spectrum is now possible (the MRS can be operated in a charged-particle mode, which involves removing the conversion foil near the implosion[5] and operating the system like a normal charged-particle spectrometer). Since both ρR and ρR symmetry are important measures of the performance of a cryogenic DT implosion, the MRS adds significantly to the existing ρR-diagnostic suite on OMEGA (Fig. 117.18).

For a fuel ρR around 100 mg/cm^2, about 1% of the primary DT neutrons elastically scatter off the deuterium, producing KOd's with energies up to 12.5 MeV as expressed by the reaction

$$\mathrm{n}(14.1\ \mathrm{MeV}) + \mathrm{D} \rightarrow \mathrm{n}' + \mathrm{D}'(\leq 12.5\ \mathrm{MeV}). \qquad (1)$$

At this neutron energy, the differential cross section for the nD-elastic scattering in the central-mass system is well known and represents the birth spectrum of the KOd's (see Fig. 117.19). As the KOd's pass through the high-density DT fuel, they lose energy in proportion to the amount of material through which they pass (ρR). A ρR value for the portion of the implosion

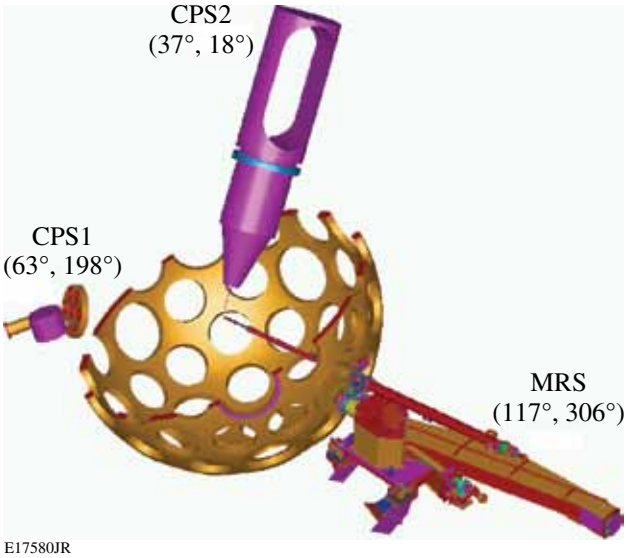

Figure 117.18
The magnetic recoil spectrometer (MRS) and the charged-particle spectrometers CPS1 and CPS2 on the OMEGA chamber. These spectrometers are used to simultaneously measure spectra of elastically scattered deuterons, so-called knock-on deuterons (KOd's), from which fuel ρR and ρR asymmetries in cryogenic DT implosions can be directly inferred. The MRS can operate in either charged-particle or down-scattered neutron mode; the latter mode allows one to measure the down-scattered neutron spectrum, from which the ρR of the fuel can be inferred as well.

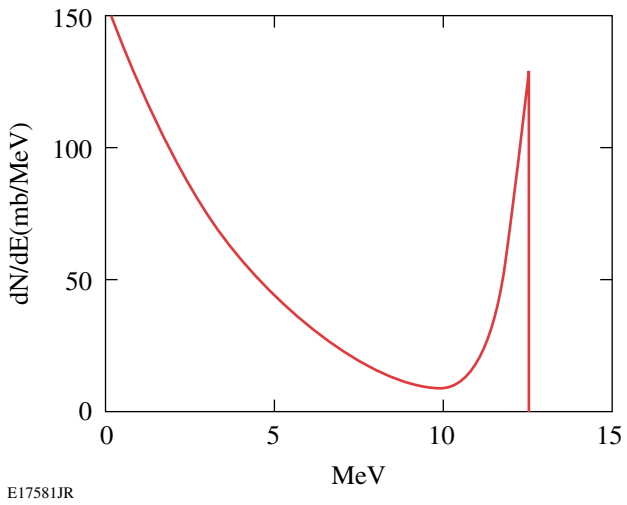

Figure 117.19
The birth spectrum of knock-on deuterons (KOd's), elastically scattered by primary 14.1-MeV neutrons. Due to kinematics, the KOd high-energy end point is at 12.5 MeV.

facing a given spectrometer can therefore be determined from the shape of the measured KOd spectrum by using theoretical formulation of the slowing down of deuteron energy in a plasma.[12] Previous work used a relatively simple model to relate the fuel ρR to the yield under the high-energy peak of the KOd spectrum.[8–10] That model, however, is subject to significant spatial-yield variations that degrade the diagnosis of the fuel ρR (spatial yield variations of about ±20% are typically observed). It also breaks down when the fuel ρR exceeds ~70 mg/cm^2 because the KOd spectrum becomes sufficiently distorted by the effects of energy slowing down that the measurement of the high-energy peak becomes ambiguous; an accurate determination of ρR must therefore rely on more-sophisticated modeling. Monte Carlo modeling of an implosion, similar to the modeling described in Ref. 7, was instead used to simulate the KOd spectrum from which a fuel ρR can be inferred. This made it possible to use more-realistic temperature and density profiles than those in the hot-spot and uniform models described in Refs. 8–10. From the Monte Carlo modeling, it was established that the shape of the KOd spectrum depends mainly on fuel ρR and that density and electron-temperature profile variations typically predicted in the high-density region play minor roles. This was concluded by studying how the spectral shape varied with varying temperature and density profiles for a fixed ρR. The variations were made to still meet a measured burn-averaged ion temperature of 2.0±0.5 keV, a radius of the high-density region of 30±10 μm, and a peak density of 10 to 160 g/cc (peak density varied less for a fixed ρR). The envelopes (represented by the standard deviation) in which the density and temperature profiles were varied are illustrated in Fig. 117.20 for a fuel ρR of 105 mg/cm^2. The resulting simulated birth profiles of the primary neutrons and KOd's are also shown in Fig. 117.20. Figure 117.21 shows how the simulated KOd spectrum varies with varying ρR. The error bars (standard deviation) shown in each spectrum represent the effect of varying density and temperature profiles, and as indicated by the error bars, the shape of the KOd spectrum depends weakly on any profile variations. In contrast, the spectral shape depends strongly on ρR. In addition, the modeling was constrained strictly by isobaric conditions at bang time, burn duration, DT-fuel composition, and a steady state during burn. As discussed in Ref. 13, the latter constraint is an adequate approximation for these types of measurements since the time evolution of the fuel ρR does not affect significantly the shape of the burn-averaged spectrum, which simplifies the ρR interpretation of the measured KOd spectrum. Multidimensional features could, on the other hand, affect the analysis and interpretation of the KOd spectrum since these effects would manifest themselves

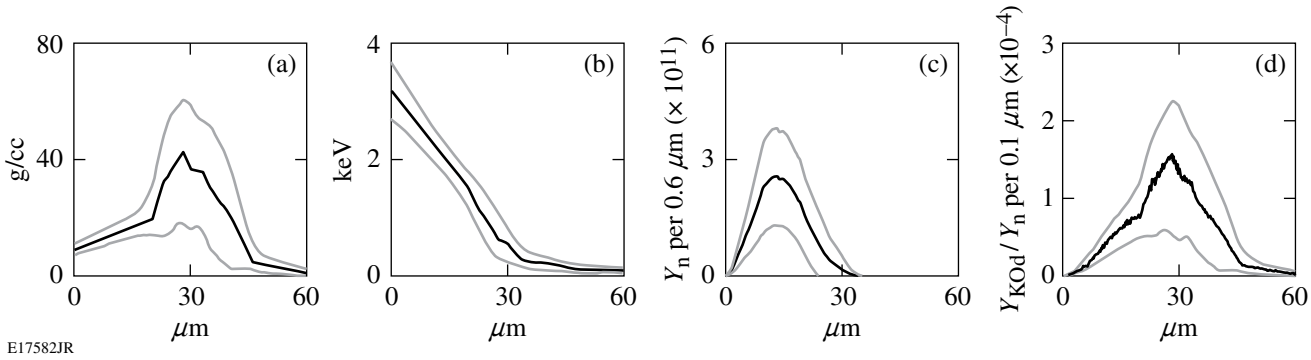

Figure 117.20
(a) Density and (b) temperature profiles used to model a cryogenic DT implosion with a ρR of 105 mg/cm^2. The black line represents the average, while the gray lines indicate the envelopes (represented by the standard deviation) in which the density and temperature profiles were varied. The variations were made to still meet the measured burn-averaged ion temperature of 2.0±0.5 keV and the position of the high-density region of 30±10 μm. Resulting birth profiles of the primary neutrons and KOd's are shown in (c) and (d). In addition, the modeling was constrained by isobaric conditions at bang time, burn duration, DT-fuel composition, and steady state during burn.

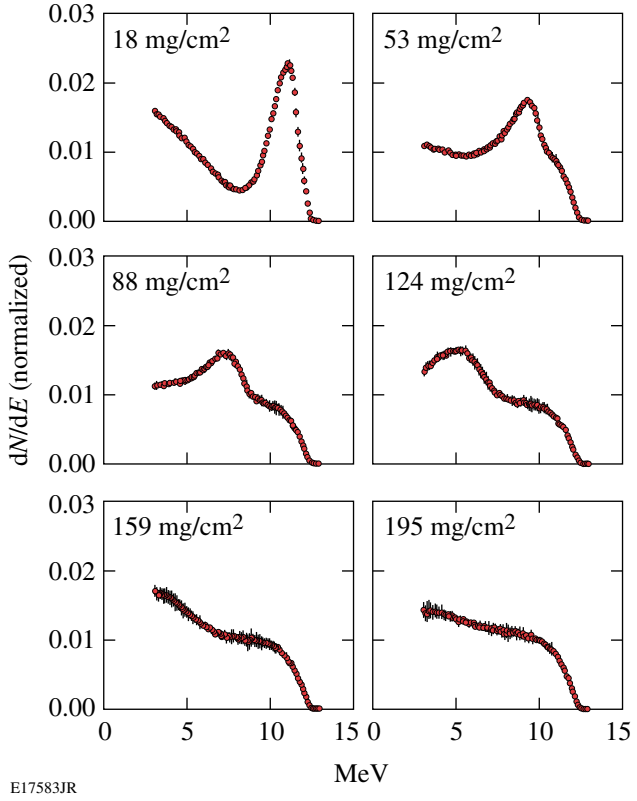

Figure 117.21
KOd spectra for different fuel ρR's. The error bars (standard deviation) shown in each spectrum represent the effect of varying density and temperature profiles. As illustrated, the shape of the KOd spectrum depends strongly on ρR, while density and temperature profile effects play minor roles as indicated by the error bars. The KOd spectra are normalized to unity.

by slightly smearing out the high-energy peak for low fuel ρR's (<100 mg/cm^2). For higher ρR's (>150 mg/cm^2), these effects should be less prominent since high-mode nonuniformities would not significantly alter the shape of the KOd spectrum.

Experiments, Data Analysis, and Results

The cryogenic DT-capsule implosions discussed in this article were driven with a laser pulse designed to keep the fuel on an adiabat α of approximately 1 to 3, where α is the ratio of the internal pressure to the Fermi-degenerate pressure.[14] The on-capsule laser energy varied from 12 to 25 kJ, and the laser intensity varied from 3×10^{14} to 10^{15} W/cm^2. Full single-beam smoothing was applied during all pulses by using distributed phase plates (DPP's),[15] polarization smoothing (PS) with birefringent wedges,[16] and 2-D, single-color-cycle, 1-THz smoothing by spectral dispersion (SSD).[17] The ablator was typically made of 5 to 10 μm of deuterated polyethylene (CD), which was permeation filled with an equimolar mixture of DT gas to 1000 atm. At this pressure, the shell and gas were slowly cooled to a few degrees below the DT triple point (19.8 K), typically producing a DT-ice layer of 90- to 100-μm thickness,[14] which is thicker than the OMEGA design energy scaled from the baseline direct-drive-ignition design for the NIF. The thicker DT ice was chosen to increase the shell stability during the acceleration phase of the implosion. In addition, by tailoring the adiabat in the shell and fuel, the expected imprint perturbation growth for such a thick shell is substantially reduced, further improving the implosion performance. Based on 1-D hydrocode simulations,[18] the burn-averaged fuel ρR is in excess of 200 mg/cm^2 for these types of implosions.

Figure 117.22 shows examples of measured and fitted simulated KOd spectra for four different low-adiabat cryogenic DT implosions. From the simulated fits to the measured spectra, ρR values ranging from 25 to 205 mg/cm^2 were inferred. The relatively low ρR's for shots 43070 and 43945 are primarily attributed to a nonoptimal-designed laser pulse shape that generated mistimed shocks. The performance of these implosions was also further degraded by the relatively large capsule offset of ~30 to 40 μm from target chamber center. Although the offset was about the same for shot 49035, the inferred ρR is significantly higher than for shots 43070 and 43945—a consequence of a better-designed laser pulse shape. The high ρR value for shot 48734 was achieved using the shock-ignition concept described in Refs. 19 and 20. The fact that the capsule was perfectly centered (11±15 μm) resulted in a determined ρR value close to the 1-D simulated value of about 200 mg/cm^2. In addition, it is notable that the high-energy endpoints are at the theoretical maximum of 12.5 MeV, demonstrating that KOd's are produced in the outermost parts of the implosion and the plastic ablator has been burnt away entirely.

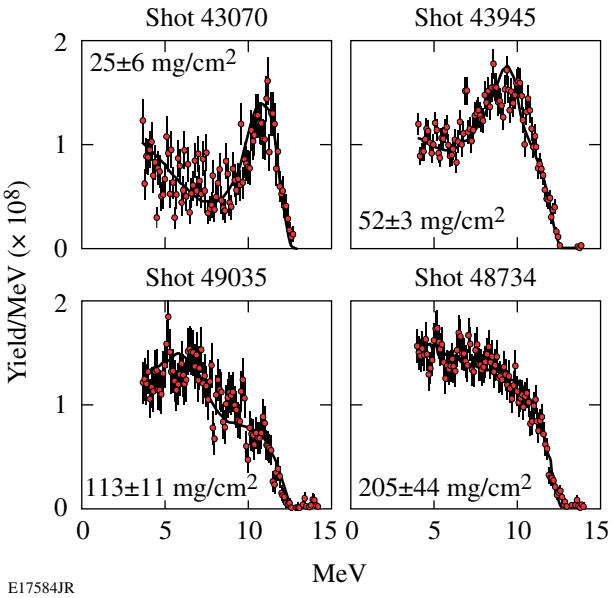

Figure 117.22
Examples of measured KOd spectra for four different low-adiabat, cryogenic DT implosions. Simulated fits (solid lines) to the measured spectra are also shown. From the fits, a fuel ρR of 25±6, 52±3, 113±11, and 205±44 mg/cm^2 was determined for shots 43070, 43945, 49035, and 48734, respectively. The errors of the inferred ρR values are due mainly to modeling uncertainties as discussed in this article and statistical uncertainties in the experimental data. See text for more detailed information about these implosions.

The ρR data obtained for hydrodynamically equivalent cryogenic D_2 implosions[14] were used to validate the ρR analysis of the KOd spectrum. Since a well-established ρR diagnostic technique exists for cryogenic D_2 implosions,[21] this comparison provides a good check of the analysis method described herein. The comparison is made in Fig. 117.23, which illustrates the experimental ρR as a function of 1-D predicted ρR [Fig. 117.23(a)] and the observed ρR_{asym} as a function of capsule offset [Fig. 117.23(b)] for low-adiabat DT and D_2 implosions driven at various intensities. Both sets of data show similar behavior, demonstrating that the ρR analysis of the KOd spectrum is accurate.

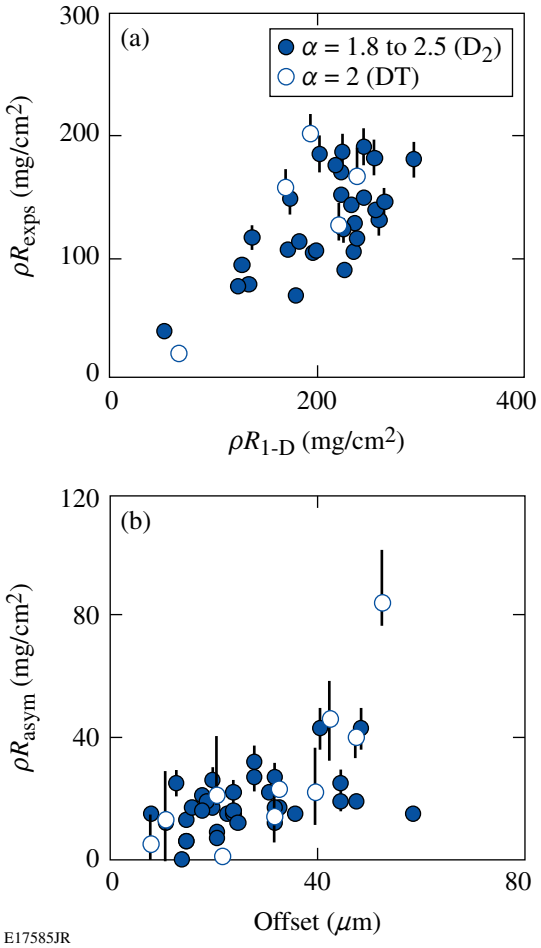

Figure 117.23
(a) Observed average ρR as a function of 1-D predicted ρR for implosions with a capsule offset of less than 40 μm to the target chamber center. (b) Observed ρR_{asym} as a function of capsule offset. These data sets are for low-adiabat DT (open data points) and D_2 (solid data points) implosions driven at various intensities. Similar performance relative to 1-D and similar ρR_{asym} as a function of capsule offset are observed for both the DT and D_2 implosions, indicating that the ρR analysis of the KOd spectrum is accurate.

Summary and Conclusions

Through Monte Carlo modeling of a cryogenic DT implosion it has been demonstrated that ρR's for moderate-ρR (<200 mg/cm^2) cryogenic DT implosions on OMEGA can be determined accurately from the shape of the measured KOd spectrum. Results from the Monte Carlo modeling of an implosion have provided a deeper understanding of the relationship between ρR, implosion structure, and KOd production. In particular, it was established that the shape of the KOd spectrum depends mainly on ρR, and that effects of spatially varying density and temperature profiles play minor roles. It should be pointed out that multidimensional features could have an effect on the analysis and interpretation of the KOd spectrum since these effects would manifest themselves by slightly smearing out the high-energy peak for low fuel ρR's (<100 mg/cm^2). For higher ρR's (>150 mg/cm^2), these effects should be less prominent since high-mode nonuniformities would not significantly alter the shape of the KOd spectrum. The ρR analysis of the KOd spectrum was also validated by comparing these results to ρR data obtained for hydrodynamically equivalent cryogenic D_2 implosions using a well-established ρR diagnostic technique. The good agreement observed between the two analysis methods indicates that the KOd analysis method described herein is accurate.

ACKNOWLEDGMENT

The work described here was supported in part by the U.S. Department of Energy (Grant No. DE-FG03-03SF22691), LLE (No. 412160-001G), LLNL (No. B504974), and GA under DOE (DE-AC52-06NA27279). This work was also supported by the U.S. Department of Energy Office of Inertial Confinement Fusion under Cooperative Agreement No. DE-FC52-08NA28302, the University of Rochester, and the New York State Energy Research and Development Authority. The support of DOE does not constitute an endorsement by DOE of the views expressed in this article.

REFERENCES

1. T. R. Boehly, D. L. Brown, R. S. Craxton, R. L. Keck, J. P. Knauer, J. H. Kelly, T. J. Kessler, S. A. Kumpan, S. J. Loucks, S. A. Letzring, F. J. Marshall, R. L. McCrory, S. F. B. Morse, W. Seka, J. M. Soures, and C. P. Verdon, Opt. Commun. **133**, 495 (1997).

2. G. H. Miller, E. I. Moses, and C. R. Wuest, Nucl. Fusion **44**, S228 (2004).

3. P. W. McKenty, V. N. Goncharov, R. P. J. Town, S. Skupsky, R. Betti, and R. L. McCrory, Phys. Plasmas **8**, 2315 (2001).

4. J. A. Frenje, K. M. Green, D. G. Hicks, C. K. Li, F. H. Séguin, R. D. Petrasso, T. C. Sangster, T. W. Phillips, V. Yu. Glebov, D. D. Meyerhofer, S. Roberts, J. M. Soures, C. Stoeckl, K. Fletcher, S. Padalino, and R. J. Leeper, Rev. Sci. Instrum. **72**, 854 (2001).

5. J. A. Frenje, D. T. Casey, C. K. Li, J. R. Rygg, F. H. Séguin, R. D. Petrasso, V. Yu. Glebov, D. D. Meyerhofer, T. C. Sangster, S. Hatchett, S. Haan, C. Cerjan, O. Landen, M. Moran, P. Song, D. C. Wilson, and R. J. Leeper, Rev. Sci. Instrum. **79**, 10E502 (2008).

6. V. Yu. Glebov, D. D. Meyerhofer, T. C. Sangster, C. Stoeckl, S. Roberts, C. A. Barrera, J. R. Celeste, C. J. Cerjan, L. S. Dauffy, D. C. Eder, R. L. Griffith, S. W. Haan, B. A. Hammel, S. P. Hatchett, N. Izumi, J. R. Kimbrough, J. A. Koch, O. L. Landen, R. A. Lerche, B. J. MacGowan, M. J. Moran, E. W. Ng, T. W. Phillips, P. M. Song, R. Tommasini, B. K. Young, S. E. Caldwell, G. P. Grim, S. C. Evans, J. M. Mack, T. Sedillo, M. D. Wilke, D. C. Wilson, C. S. Young, D. Casey, J. A. Frenje, C. K. Li, R. D. Petrasso, F. H. Séguin, J. L. Bourgade, L. Disdier, M. Houry, I. Lantuejoul, O. Landoas, G. A. Chandler, G. W. Cooper, R. J. Lepeer, R. E. Olson, C. L. Ruiz, M. A. Sweeney, S. P. Padalino, C. Horsfield, and B. A. Davis, Rev. Sci. Instrum. **77**, 10E715 (2006).

7. S. Kurebayashi, J. A. Frenje, F. H. Séguin, J. R. Rygg, C. K. Li, R. D. Petrasso, V. Yu. Glebov, J. A. Delettrez, T. C. Sangster, D. D. Meyerhofer, C. Stoeckl, J. M. Soures, P. A. Amendt, S. P. Hatchett, and R. E. Turner, Phys. Plasmas **12**, 032703 (2005).

8. S. Skupsky and S. Kacenjar, J. Appl. Phys. **52**, 2608 (1981).

9. S. Kacenjar, S. Skupsky, A. Entenberg, L. Goldman, and M. Richardson, Phys. Rev. Lett. **49**, 463 (1982).

10. C. K. Li, F. H. Séguin, D. G. Hicks, J. A. Frenje, K. M. Green, S. Kurebayashi, R. D. Petrasso, D. D. Meyerhofer, J. M. Soures, V. Yu. Glebov, R. L. Keck, P. B. Radha, S. Roberts, W. Seka, S. Skupsky, C. Stoeckl, and T. C. Sangster, Phys. Plasmas **8**, 4902 (2001).

11. F. H. Séguin, J. A. Frenje, C. K. Li, D. G. Hicks, S. Kurebayashi, J. R. Rygg, B.-E. Schwartz, R. D. Petrasso, S. Roberts, J. M. Soures, D. D. Meyerhofer, T. C. Sangster, J. P. Knauer, C. Sorce, V. Yu. Glebov, C. Stoeckl, T. W. Phillips, R. J. Leeper, K. Fletcher, and S. Padalino, Rev. Sci. Instrum. **74**, 975 (2003).

12. C. K. Li and R. D. Petrasso, Phys. Rev. Lett. **70**, 3059 (1993).

13. J. A. Frenje, C. K. Li, J. R. Rygg, F. H. Séguin, D. T. Casey, R. D. Petrasso, J. Delettrez, V. Yu. Glebov, T. C. Sangster, O. Landen, and S. Hatchett, Phys. Plasmas **16**, 022702 (2009).

14. T. C. Sangster, R. Betti, R. S. Craxton, J. A. Delettrez, D. H. Edgell, L. M. Elasky, V. Yu. Glebov, V. N. Goncharov, D. R. Harding, D. Jacobs-Perkins, R. Janezic, R. L. Keck, J. P. Knauer, S. J. Loucks, L. D. Lund, F. J. Marshall, R. L. McCrory, P. W. McKenty, D. D. Meyerhofer, P. B. Radha, S. P. Regan, W. Seka, W. T. Shmayda, S. Skupsky, V. A. Smalyuk, J. M. Soures, C. Stoeckl, B. Yaakobi, J. A. Frenje, C. K. Li, R. D. Petrasso, F. H. Séguin, J. D. Moody, J. A. Atherton, B. D. MacGowan, J. D. Kilkenny, T. P. Bernat, and D. S. Montgomery, Phys. Plasmas **14**, 058101 (2007).

15. Y. Lin, T. J. Kessler, and G. N. Lawrence, Opt. Lett. **20**, 764 (1995).

16. T. R. Boehly, V. A. Smalyuk, D. D. Meyerhofer, J. P. Knauer, D. K. Bradley, R. S. Craxton, M. J. Guardalben, S. Skupsky, and T. J. Kessler, J. Appl. Phys. **85**, 3444 (1999).

17. S. Skupsky, R. W. Short, T. Kessler, R. S. Craxton, S. Letzring, and J. M. Soures, J. Appl. Phys. **66**, 3456 (1989).

18. J. Delettrez, Can. J. Phys. **64**, 932 (1986).

19. R. Betti, C. D. Zhou, K. S. Anderson, L. J. Perkins, W. Theobald, and A. A. Solodov, Phys. Rev. Lett. **98**, 155001 (2007).

20. W. Theobald, R. Betti, C. Stoeckl, K. S. Anderson, J. A. Delettrez, V. Yu. Glebov, V. N. Goncharov, F. J. Marshall, D. N. Maywar, R. L. McCrory, D. D. Meyerhofer, P. B. Radha, T. C. Sangster, W. Seka, D. Shvarts, V. A. Smalyuk, A. A. Solodov, B. Yaakobi, C. D. Zhou, J. A. Frenje, C. K. Li, F. H. Séguin, R. D. Petrasso, and L. J. Perkins, Phys. Plasmas **15**, 056306 (2008).

21. F. H. Séguin, C. K. Li, J. A. Frenje, S. Kurebayashi, R. D. Petrasso, F. J. Marshall, D. D. Meyerhofer, J. M. Soures, T. C. Sangster, C. Stoeckl, J. A. Delettrez, P. B. Radha, V. A. Smalyuk, and S. Roberts, Phys. Plasmas **9**, 3558 (2002).